

Article

Selective scandium (Sc) extraction from bauxite residue (red mud) obtained by alkali fusion-leaching method

Andrei Shoppert^{1,*}, Irina Loginova², Julia Napol'skikh², Aleksey Kyrchikov², Leonid Chaikin², Denis Rogozhnikov¹ and Dmitry Valeev³

¹ Laboratory of Advanced Technologies in Non-ferrous and Ferrous Metals Raw Materials Processing, Ural Federal University, 620002 Yekaterinburg, Russia, darogozhnikov@yandex.ru (D.R.)

² Department of Non-ferrous Metals Metallurgy, Ural Federal University, 620002 Yekaterinburg, Russia; i.v.loginova@urfu.ru (I.L.); anapolskikh512@gmail.com (J.N.); akirchikov@yandex.ru (A.K.); l.i.chaikin@urfu.ru (L.C.)

³ Laboratory of sorption methods, Vernadsky Institute of Geochemistry and Analytical Chemistry of the Russian Academy of Sciences, 119991, Moscow, Russia; dmvaliev@yandex.ru (D.V.)

* Correspondence: a.a.shoppert@urfu.ru (A.S.)

Abstract: One of the potential sources of rare-earth elements (REEs) is the solid waste from alumina industry - bauxite residue, known as "red mud" (RM). The main REEs from the raw bauxite are concentrated in RM after the Bayer leaching process. The earlier worldwide studies were focused on the scandium (Sc) extraction from RM by concentrated acids to enhance the extraction degree. This leads to the dissolution of major oxides (Fe_2O_3 and Al_2O_3) from RM. This article studies the possibility of selective Sc extraction from alkali fusion red mud (RMF) by diluted nitric acid (HNO_3) leaching at $\text{pH} \geq 2$ to prevent co-dissolution of Fe_2O_3 . RMF samples have been analyzed by X-ray fluorescence spectrometry (XRF), X-ray diffraction (XRD), electron probe microanalysis (EPMA), and inductively coupled plasma mass spectrometry (ICP-MS). Sc extraction has been found to be 71.2 % at RMF leaching by HNO_3 at $\text{pH}=2$ and at 80 °C during 90 min. The kinetic analysis of experimental data by the shrinking core model has shown that Sc leaching process is limited by the interfacial diffusion and the diffusion through the product layer. The apparent activation energy (E_a) was 19.5 kJ/mol. We have established that according to EPMA of RMF, Sc is associated with iron minerals; it could act as the product layer. The linear dependence of Sc extraction of magnesium (Mg) extraction has been revealed. This fact indicates that Mg can act as a leaching agent of Sc presented in RMF by ion-exchangeable phase.

Keywords: bauxite residue; red mud; scandium; acid leaching; kinetics; shrinking core model; waste utilization.

1. Introduction

Red mud (RM) is a solid waste generated by alkali (NaOH) leaching of bauxite by Bayer process for alumina production [1]. More than one ton of RM is produced for one ton of alumina (Al_2O_3). Annually more than 150 Mt of RM are stored in landfills and sea [2]. The RM utilization degree is extremely low due to the high Na, Al, Si, Ca content [3]. The high content of toxic metals (Na, Si, Cd, Ni, As, Sb, Pb, Cr) and small particle size of RM ($< 10 \mu\text{m}$) lead to contamination of soil, air, and water around the landfills [4,5].

In addition to RM obtained by the Bayer process, there is a sintering RM. It is obtained during sintering high-silica bauxite with soda (Na_2CO_3) and limestone (CaCO_3) and further water leaching [6]. The sintering RM contains less caustic alkali (not more 5 wt%) [7], but its CaO content is much higher (up to 42 wt%) [8]. This type of RM can generally be utilized during production of construction materials due to low iron oxide (Fe_2O_3) content and a high content of CaO and SiO_2 [9]. Alumina refineries that use combined methods - Bayer and sintering (Urals Alumina Refinery and Bogoslovsk Alumina Refinery in Russia) usually store both types of waste on one landfill [10,11].

Despite the method of obtaining, RM contains high number of valuable components, especially REEs that are widely used in high-tech materials production [12–14]. RM high content of REEs is explained by the following: REEs do not dissolve during bauxite alkali leaching; they concentrate in the solid residue [15,16]. Main studies on the REEs extraction from RM are devoted to scandium (Sc) extraction.

The Sc demand annually increases as it is used in lasers glass, catalysts, electronic components, halide lamps, fuel cells, and non-ferrous metallurgy [17]. The most relevant application is the production of Al-Sc alloys with high strength and low weight [18]. The Sc content in different types of RM (more than 100 mg kg⁻¹) is higher than the average abundance in the Earth's crust (22 mg kg⁻¹) [19]. The huge amount of accumulated RM (more than 4 Bt) [20] can be used as raw material for the Sc extraction.

One of the promising and eco-friendly methods for the Sc extraction is sodium bicarbonate (NaHCO₃) leaching [21,22] and carbonization [23]. UC RUSAL launched a pilot plant by NaHCO₃ leaching in 2014 [24]. However, the Sc extraction degree by this method does not exceed 30-40%, even at application of the sorption in pulp process [25].

The most effective methods for Sc extraction are RM leaching by dilute inorganic acids [26–29]. Rivera et al. found that for a high Sc extraction degree, complete iron oxide leaching is also necessary [30]. Sc is primarily associated with iron minerals in RM in the form of ions that are adsorbed on the minerals surface or replace other ions in solid matrix [31]. High iron content in the acid solution complicates the subsequent Sc extraction since these metals have similar physical and chemical properties [17].

Ochsenkuehn-Petropoulou et. al. [27,32] showed that the Sc extraction from the sintering RM can be carried out at a pH > 1.5. This reduces the Fe extraction; however, consumption of acid is large due to reaction with CaO. Anawati et al. [33] found that it is possible to increase Sc extraction by fusing RM with sulfuric acid or alkali. During the RM fusing iron minerals undergo phase transformation that can lead to the liberation of REEs from the solid matrix of the minerals. Therefore, the obtaining of RM by fusing may provide an alternative for the selective extraction of REEs without Fe, Al and Ca co-dissolution.

In this research, we studied the selective Sc extraction from RM obtained by fusing bauxite with NaOH to optimize the leaching process at pH > 2. A diluted nitric acid was chosen as the leaching agent since Reid et al. [34] showed that the Sc extraction degree in this case was higher. The influence of pH, the liquid to solid ratio (L:S), temperature, and leaching time on Sc extraction have been investigated. The mechanism and kinetics of leaching have been studied using the shrinking core model.

2. Materials and methods

2.1. Analysis

The phase composition of RM was detected by powder X-ray diffraction spectrometry (XRD) with a Rigaku D/MAX-2200 diffractometer (Rigaku Co., Japan) using a Cu-K α radiator ($\lambda = 1.541841 \text{ \AA}$) and a PDF-2 database (International Center for Diffraction Data). Chemical analysis of the major elements in RM was performed by powder X-ray fluorescence spectrometry (XRF) with an Axios MAX spectrometer (Malvern Panalytical Ltd., Almelo, Netherlands). Chemical analysis of the trace elements was analyzed by inductively coupled plasma mass spectrometry (ICP-MS, PerkinElmer NexION 300S instrument, Waltham, MA, USA). The scanning electron microscopy (SEM) images were taken to determine the morphology of RM particles (JEOL JSM-6390, Tokyo, Japan). Electron probe micro-analysis (EPMA) was performed using a Cameca SX 100 microanalyzer (CAMECA Instruments, Inc., Madison, WI, USA) equipped with an energy-dispersive X-ray spectroscopy analysis (EDS) module Bruker XFlash 6 (Bruker Nano GmbH, Berlin, Germany). The loss on ignition (LOI) was determined by a Diamond TG/DTA (PerkinElmer, Waltham, MA, USA), by heating an RM sample from 50 to 1000 °C at the rate of 20 °C/min.

2.2. Materials

RM sample was obtained by alkali fusion-leaching method from bauxite of Middle-Timan deposit (Ukhta, Russia). Chemical composition and properties of the raw bauxite and the red mud obtained at different fusion temperatures (RMF), as well the mechanism of the process was presented in our previous article [35]. Alkali fusion conditions used in this research were as follows: T = 300 °C, fusion time 120 min, bauxite/NaOH weight ratio 1:1. Fusing product was leached by water at T = 80 °C, L:S ratio = 3.5 and leaching time 30 min. RMF was filtered, washed by distilled water, and dried at T = 110 °C. RMF chemical composition is presented in Table 1. RMF contains a high amount of Fe and a low amount of Na, Al and Si compared to Bayer RM [35]. XRD of RMF is shown on Figure 1. Almost all iron in RMF is presented as maghemite ($\gamma\text{-Fe}_2\text{O}_3$). The latter is formed by hydrolysis of sodium ferrite (NaFeO_2), which is the main iron phase of fusion product. Some amount of hematite (Fe_2O_3) and chamosite ($(\text{Fe}^{2+},\text{Mg})_5\text{Al}(\text{AlSi}_3\text{O}_{10})$), the main phases of raw bauxite, still can be seen after fusion-leaching process.

Table 1. Chemical composition of the red mud obtained by alkali fusion-leaching method (RMF).

Major components, wt%										
Fe ₂ O ₃	TiO ₂	SiO ₂	Al ₂ O ₃	MnO	Na ₂ O	MgO	CO ₂	CaO	ZrO ₂	LOI
65.50	7.79	6.02	5.04	1.29	0.78	0.75	0.65	0.39	0.26	11.52
Minor components, mg kg ⁻¹										
CeO ₂	La ₂ O ₃		Nd ₂ O ₃		Nb ₂ O ₅		Sc ₂ O ₃		Y ₂ O ₃	
862	365		322		241		212		196	

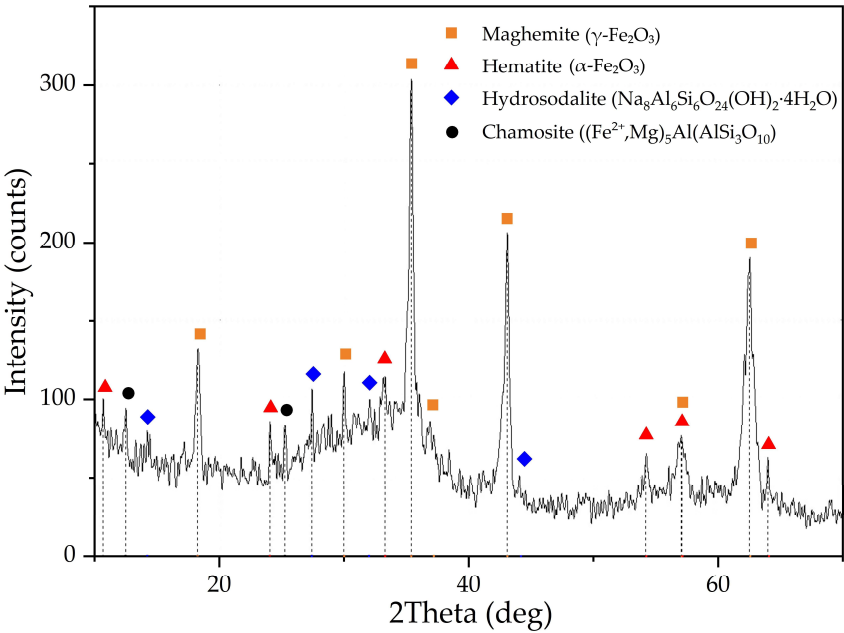


Figure 1. XRD pattern of the initial red mud obtained by alkali fusion-leaching of bauxite (RMF).

According to previous researches [36–39], Sc is commonly adsorbed on Fe_2O_3 and in the aluminosilicates channels that is formed during desilication of pregnant solution [25]. During the alkali fusion-leaching method hematite and chamosite are transformed into maghemite. Desilication product (DSP), in this case, is hydrosodalite ($\text{Na}_8\text{Al}_6\text{Si}_6\text{O}_{24}(\text{OH})_2 \cdot 4\text{H}_2\text{O}$). DSP amount is very low, as can be seen from Table 1 and Figure 1. Therefore, Sc could be liberated from the solid matrix of bauxite minerals; it is not included in DSP. However, scandium could be adsorbed on the Fe_2O_3 after alkali fusion-leaching method. This fact could lead to an increased REEs extraction compared to

Bayer RM treatment. The EPMA analysis showed the association of Sc with main components in RMF (Figure 2). The mapping analysis confirms that Sc is associated more with Fe_2O_3 than with other minerals. Figure 3 shows the SEM images of RMF and Bayer RM, obtained from Middle Timan bauxite treatment on Urals Alumina Refinery. It could be seen on Figure 3 that RMF consists of small particles of approximately the same size of several microns or less. The Bayer RM particles are larger; this RM consists of particles of different sizes (0.2- 5 μm).

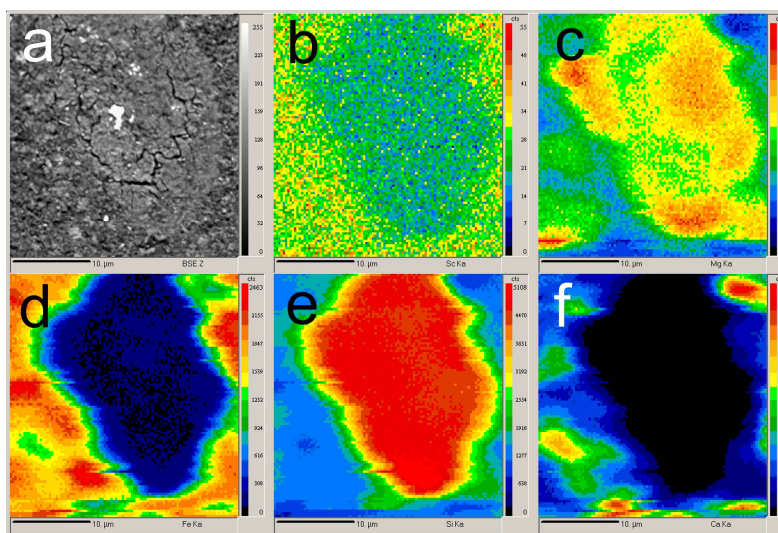


Figure 2. EMPA of the initial red mud obtained by alkali fusion-leaching of bauxite (RMAF): BSE image of the RMAF surface (a); mapping of the Sc distribution (b); mapping of the Mg distribution (c); mapping of the Fe distribution (d); mapping of the Si distribution (e); mapping of the Ca distribution (f).

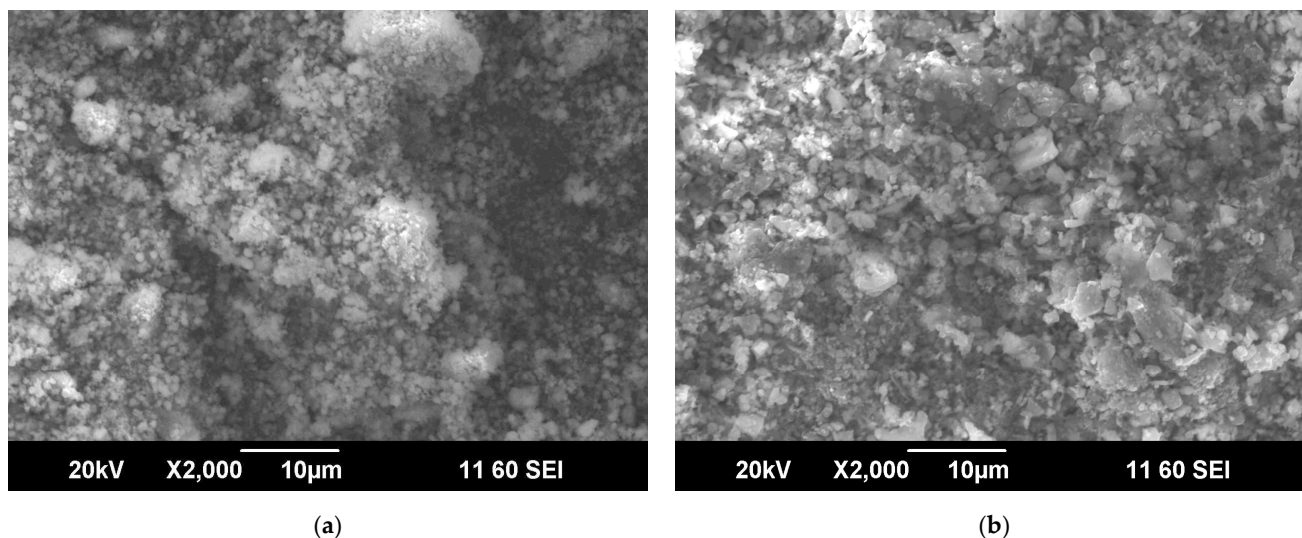


Figure 3. SEM images of the initial red mud obtained by alkali fusion-leaching of bauxite (RMF) (a) and the Bayer red mud obtained from Middle Timan bauxite treatment on Urals Alumina Refinery (b).

2.3. Experiments

The leaching of RMF in diluted nitric acid (HNO_3) was carried out in a 0.5 L thermostatic reactor "Lenz Minni" (Lenz Laborglas GmbH & Co. KG, Wertheim, Germany) fitted with an overhead stirrer. The 10, 15 or 20 g of RMF was mixed into the 180 mL of

distilled water, then 20 mL of HNO_3 solution with the predetermined concentration was added, according to the RMF sample weight and desired pH. The pH of the solution was kept constant by addition of 1M HNO_3 solution using Automatic titrator ATP-02 (JSC Akvilon, Russia).

After leaching, the solid residue was separated from the acid solution by filtration on a Buchner funnel. The Sc, Fe, Al, and Mg content in the solution were measured using ICP-OES. After washing and drying of the solid residue for 8 h at $T = 110^\circ\text{C}$, it was used for SEM and XRF analysis.

The metals extraction degree was calculated by the following Equation 1:

$$\eta_{\text{Me}} = C_{\text{Me}} \times V \times 100\% / (m \times X_{\text{Me}}), \quad (1)$$

where C_{Me} is the concentration of a metal in the solution (mg L^{-1}), V is the volume of the solution (L), m is the mass of RMF (kg), X_{Me} is a content of a metal in RMF (mg kg^{-1}).

The Eh-pH diagrams were calculated using the HSC Chemistry Software v. 9.9 (Outokumpu Research Oy, Finland).

3. Results and discussion

3.1. Effect of leaching conditions on the Sc selective leaching from RMF

Selective Sc leaching was achieved due to the difference of the Sc and Fe solubility at $\text{pH} > 2$. Thermodynamics in the system Fe-H-O and Sc-H-O at 25°C at different pH levels are shown in Figure 4. At pH 1.2 to 3 and high Eh (> 0.5) $\text{Fe}(\text{OH})_3$ begins to precipitate. Unlike Fe, Sc begins to precipitate only at pH 6. In addition, kinetics of Fe and Sc minerals leaching should be considered. Rivera et al. [19] showed that Sc extraction from industrial bauxite residue is very low at $\text{pH} > 2.5$. Thus, it is necessary to use concentrated acid solutions for complete Sc leaching. Accordingly, Fe extraction degree is high at this condition.

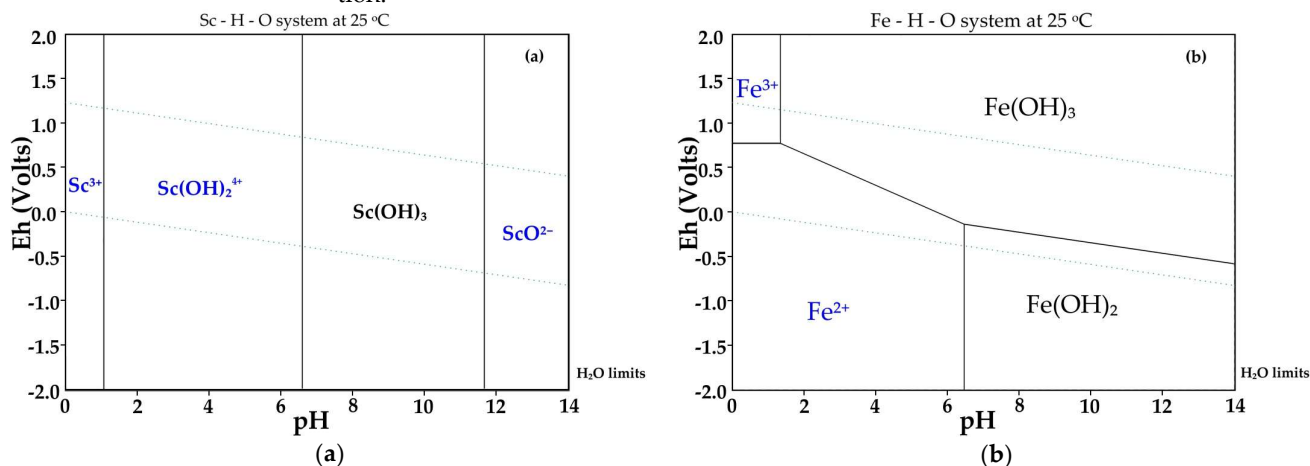


Figure 4. Thermodynamic modeling of the system Sc-H-O at 25°C (a); and the system Fe-H-O (b).

The optimal pH range was defined as 2-3.5 for a better Sc extraction selectivity and leaching rate. The effect of temperature (T , $^\circ\text{C}$), leaching time (τ , min), pH, liquid to solid ratio (L:S) on the Sc extraction with HNO_3 from RMF is shown in Figure 5. Pareto chart was constructed to estimate standardized effect of each parameter on Sc extraction (Figure 5d).

As Figure 5a shows, the Sc extraction increases by 10-15 % with an increase in time from 10 to 90 min at all temperatures. An increase in temperature from 60 to 80°C after 90 min of leaching leads to an increase in Sc extraction by 12 %. The low effect of leaching time and temperature at later stages of leaching (when $>50\%$ of Sc was extracted) could be a sign of the diffusion limitation (reagent diffusion to the surface of the reaction through the product layer or the liquid film).

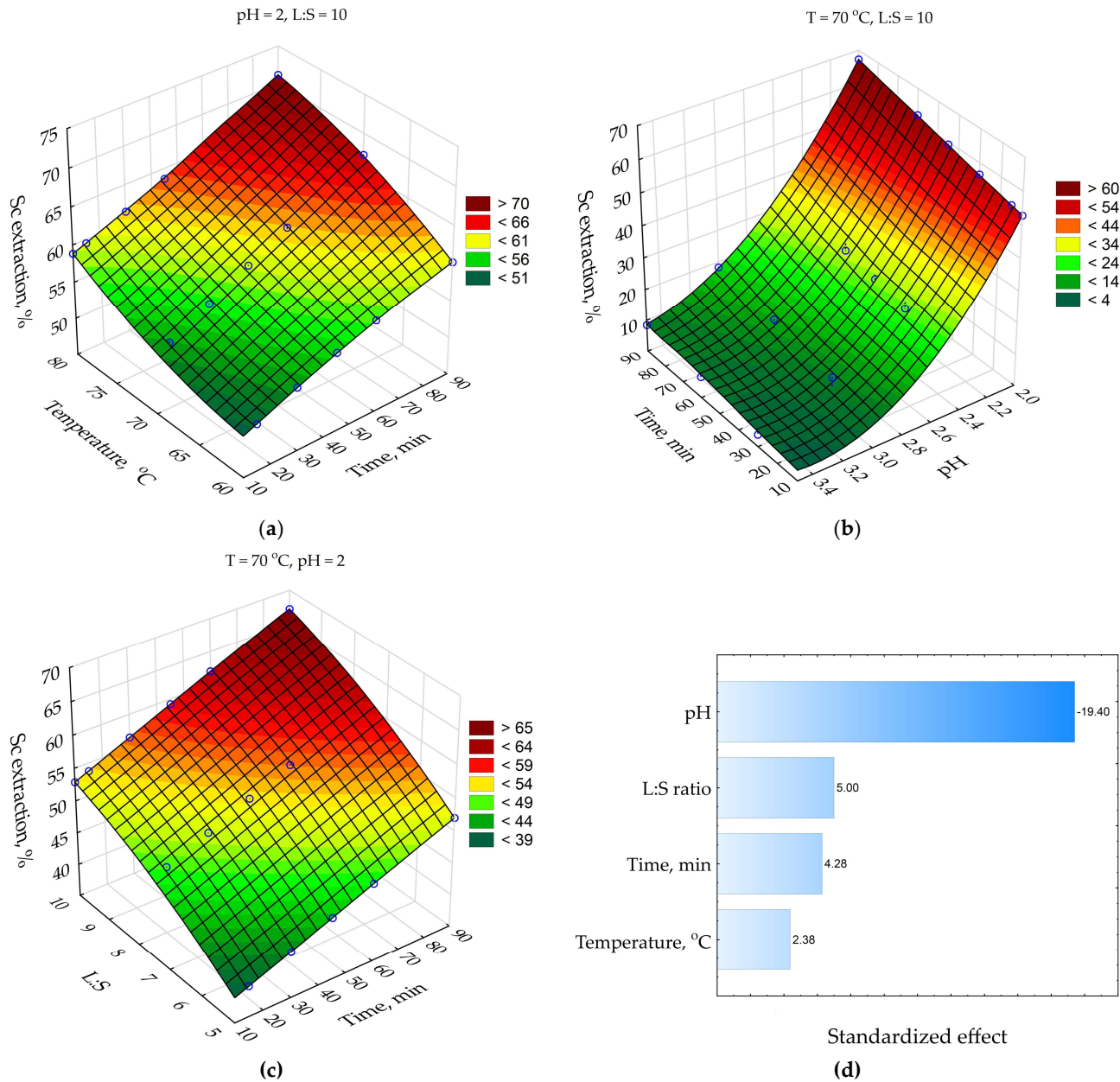


Figure 5. Response surfaces for: (a) effect of time and temperature on the Sc extraction; (b) effect of time and pH on the Sc extraction; (c) effect of time and L:S ratio on the Sc extraction; (d) Pareto chart. Blue points are the experimental data.

The pH effect on the Sc extraction is shown on Figure 5b. At high pH = 3-3.5, the Sc extraction was lower than 20 % despite leaching time, but it increases when the pH level reduces to 2-2.5. The pH decreases from 3.5 to 2 leads to an increase in Sc extraction after 90 min of leaching at $T = 70^{\circ}\text{C}$ from 10 to 68 %. Therefore, maintenance of pH is significant for a high Sc extraction from RMF. An increase in the L:S ratio from 5 to 10 also increases Sc extraction by 18% after 90 min of leaching at $T = 70^{\circ}\text{C}$ (Fig. 5c). It can be related to the high amount of free acid that react with Sc minerals. Above observations are confirmed by the Pareto chart on Figure 4d, where standardized effect of each parameter is given. The pH effect is more than four times higher than the L:S ratio and leaching time effects. The standardized effect of temperature is two times lower than leaching time.

3.2 Study of the kinetics and mechanism of Sc leaching from RMF.

The great effect of L:S ratio and low effect of temperature on the Sc extraction indicate that diffusion is the limiting stage of the leaching process. After 10 min of leaching the Sc extraction degree is already higher than 50 % at pH = 2. Therefore, at the initial time the surface chemical reaction could be the limiting stage. To determine the limiting stage, the kinetics studies at the first 5 min of leaching process were investigated.

Shrinking core model (SCM) is usually used to characterize kinetic of heterogenic leaching process [40]. SCM assumes that leaching rate is controlled by surface chemical reaction, or diffusion through the liquid film, or diffusion through the porous solid product. The unreacted core of the particle covered by this product shrinks to the center during the reaction. A several kinetic equations were used for the determination of each stage (Table 2).

Least square graphical method (Figure 6) was used to fit experimental data to each equation from Table 2. The results of fitting for Equation 3 are shown in Figure 6b.

Table 2. SCM equation fitting for Sc extraction from RMF.

#	Equation	Fitting results (R²)				
		60 °C	65 °C	70 °C	75 °C	80 °C
1	$1 - 3(1 - X)^{2/3} + 2(1 - X) = k_1\tau^*$	0.957	0.950	0.940	0.935	0.921
2	$1 - (1 - X)^{1/3} = k_2\tau$	0.733	0.724	0.712	0.706	0.687
3	$1/3\ln(1 - X) + [(1 - X)^{-1/3} - 1] = k_3\tau$	0.982	0.980	0.974	0.974	0.967

* k_i is the corresponding rate constant.

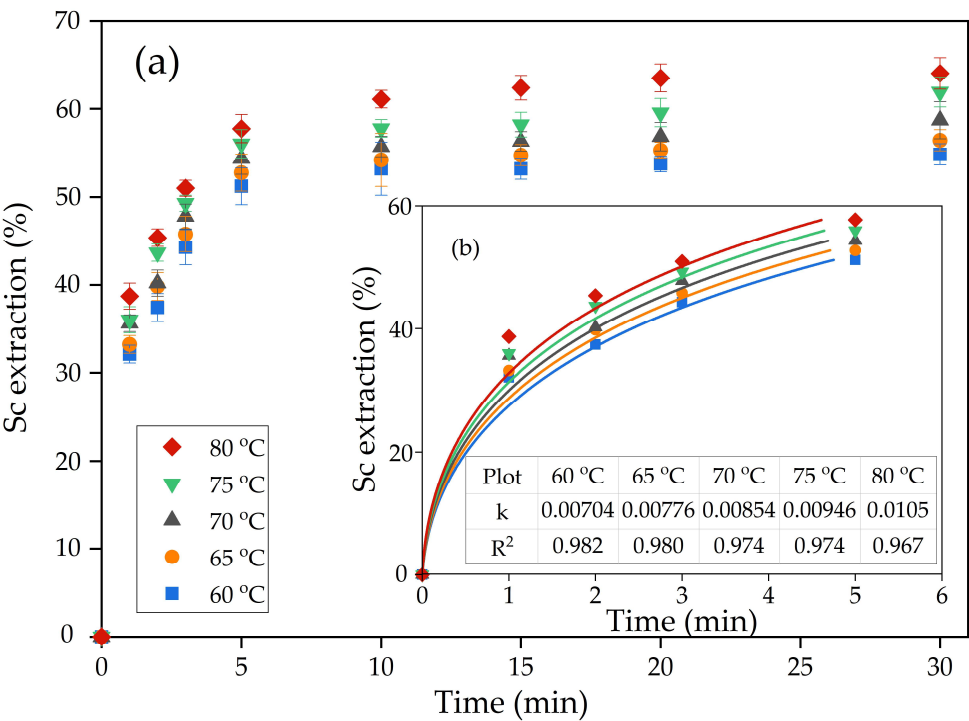


Figure 5. Dependence of the degree of scandium extraction on temperature (a); fitting of experimental data of leaching during the first 5 min to the new shrinking core model (b).

As Figure 6 and Table 2 reveal, the surface reaction equation suits less for the characterization of Sc leaching kinetics, as R^2 is < 0.8 for all temperatures. The new shrinking core model (Equation 3, Table 2) is more correct for fitting of the experimental data. This model assumes that interfacial diffusion and diffusion through the product layer are the limiting stages of the leaching process.

Arrhenius plot was created in $\ln K$ -1000/T coordinates for the further characterization of limiting stage of the leaching process (Figure 7). It applied the rate constants showed in Figure 6b. The linear fitting was performed to obtain equation $y = ax + b$ type. Where a is the slope of the curve that is used to find the apparent activation energy using Equation 3.

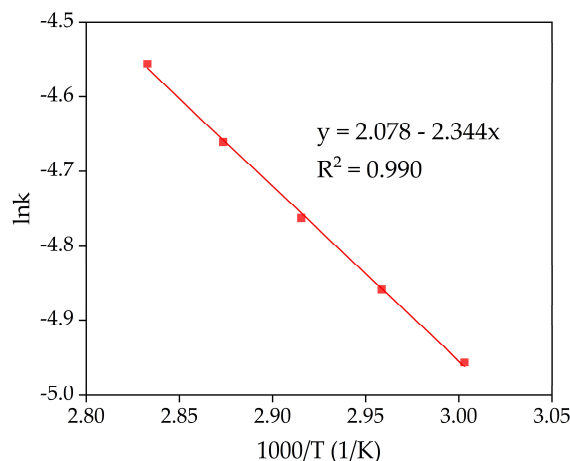


Figure 6. Dependence of $\ln K$ on $1000/T$ (Arrhenius plot) for Sc extraction from RMF at different temperatures.

The obtained value of the apparent activation energy is 19.5 kJ/mol. The shrinking core model and the value of the activation energy confirm that diffusion of the reagent to the reaction surface is the limiting stage of the Sc leaching process. The product layer that can prevent reagent diffusion to the reaction surface can be hematite or chamosite that did not react with NaOH (according to Figure 1) and remains inert in a slightly acidic condition ($\text{pH} > 2$). The maghemite particles although very fine, with a high specific surface area and porosity, could be the product layer that prevents diffusion as they are almost inert at such pH.

The experiments concerning dependence of Al, Mg and Fe extraction on Sc extraction (Figure 8) were performed for a further study of the leaching process mechanism. The experimental data was subjected to the linear and non-linear fitting using 3rd order polynomial and Boltzmann function [41]. The Boltzmann function gives a sigmoidal curve, and well suits the characterize processes with a great increase in values. According to Figure 8, the Boltzmann function $y = 81 + (1.3 - 81.0)/(1 + \exp(x - 34.9)/1.2)$ suits better ($R^2 = 0.992$) for a description of the dependence of Al extraction on Sc extraction. This can be explained by the fact that almost all Al in RMF is contained in the hydrosodalite (Figure 1). Hydrosodalite begins to dissolve at $\text{pH} > 2$, thus a great increase in the Al extraction degree is observed. According to Figure 2, the Sc amount associated with aluminosilicate is low. Petrakova et al. [25] showed that Sc associated with the DSP accounts more than 30% of Sc in Bayer RM. Therefore, the increase in aluminosilicate dissolution could raise the Sc extraction degree.

At $\text{pH} > 2$ the Fe extraction was lower than 3%, as the Sc extraction was less than 50%. According to EMPA analysis of RMF (Figure 2) and our previous research [42], it was found that the association of Sc with iron-containing minerals is high. However, after alkali-fusing of bauxite followed by water leaching the hematite matrix was destroyed. Maghemite that formed after water leaching has a high specific surface area value (55 m^2/g), so Sc can be adsorbed on its surface. Therefore, the leaching of REEs from this type of RM is more efficient. Some amount of hematite and chamosite remain in the solid residue (Figure 1), so its solid matrix should be destroyed at lower pH for Sc extraction. This fact leads to an increase in the Fe and Sc extraction. Thus, polynomial curve ($y =$

$0.111x - 0.003x^2 + 3.117 \cdot 10^{-5}x^3$) suits the best ($R^2 = 0.937$) for a description of the dependence of Fe extraction on Sc extraction, as shown in Figure 8.

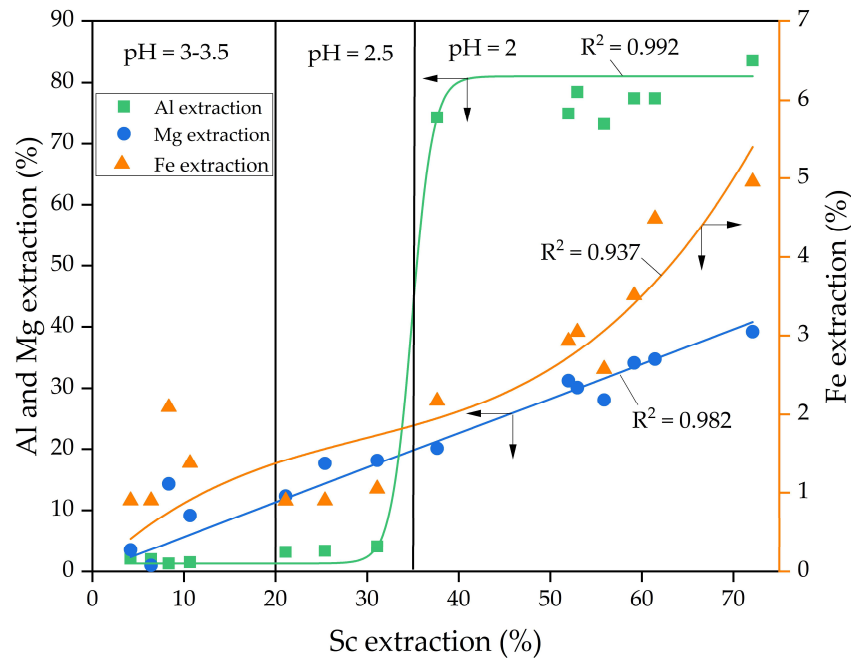


Figure 8. Dependence of the Al, Mg and Fe extraction on Sc extraction and the fitting of the experimental data obtained at different pH value.

The dependence of Mg extraction on Sc extraction was almost linear ($y = 0.565x$, with $R^2 = 0.982$). It means that the Sc extraction is associated with the Mg extraction at all pH values. However, according to EPMA analysis (Figure 2), the Sc association with Mg in RMF is low. He Q. et al. [43] showed that the ion-exchangeable phase of REEs could be easily extracted by $MgSO_4$ solutions. Therefore, it can be assumed that a high amount of Sc after the alkali fusion-leaching method is presented in RMF in the ion-exchangeable phase. At the first step, Mg is extracted into the solution in the cationic form, then Mg^{+} begins to act as a leaching agent. Thus, the linear dependence of Sc extraction on Mg extraction can be explained by this fact. Although Mg content in RMF was ~ 0.8 wt% (Table 1), it's more than 40 times higher than Sc content. The Mg extraction during the leaching process is $\sim 40\%$, however, this content of Mg in the acid solution is enough to leach more than 70 wt% of Sc. The mechanism of Sc leaching from RMF is proposed in Figure 8.

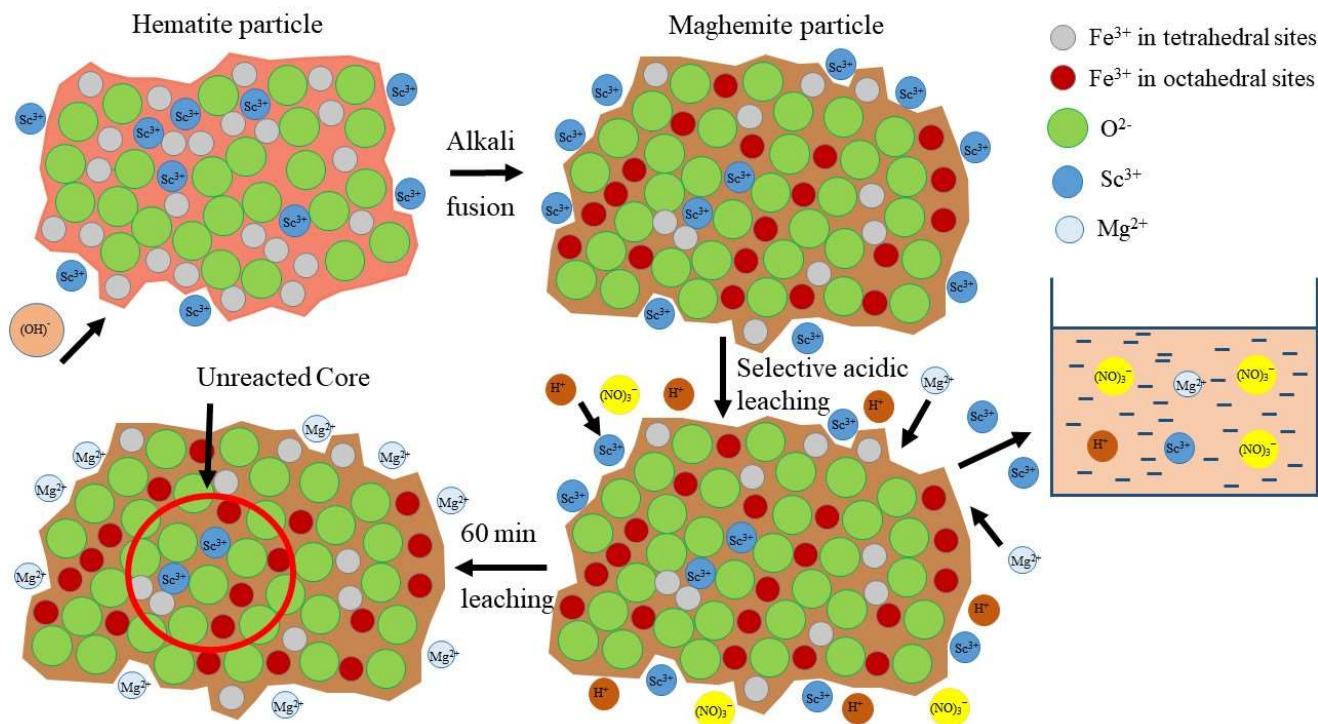


Figure 8. The mechanism of selective Sc leaching from RMF.

The Fe₂O₃ content of the solid residue after Sc extraction was >76 wt% (Table 3). The Na₂O content was lower than 1 wt%. The high content of maghemite nanoparticles with high specific surface area and low amount of other impurities determine its possible adsorption, ions-exchange, catalysts, magnetism functions [35].

Table 3. Chemical composition of the red mud after selective REE leaching at pH 2, T = 70 °C, L:S = 10 and τ = 30 min.

Major components, wt%										
Fe ₂ O ₃	TiO ₂	SiO ₂	Al ₂ O ₃	MnO	Na ₂ O	MgO	CO ₂	CaO	ZrO ₂	LOI
76.27	8.87	6.80	1.41	1.48	0.93	0.66	1.05	0.23	0.25	1.59
Minor components, mg kg ⁻¹										
CeO ₂	La ₂ O ₃		Nd ₂ O ₃		Nb ₂ O ₅		Sc ₂ O ₃		Y ₂ O ₃	
904	156		76		201		110		20	

4. Conclusions

In this article, the possibility of selective Sc leaching from RM obtained by the alkali fusion-leaching method using dilute nitric acid (pH 2-3.5) was studied. More than 70 wt% of Sc was extracted at pH = 2, T = 80 °C, L:S ratio 10, and leaching time 90 min. The Fe extraction at these conditions was lower than 5%. Using an EMPA, XRD analysis, and the shrinking core model for kinetics investigation, the following main conclusions were obtained:

1. The results of the kinetics analysis show that the Sc leaching process is limited by the interfacial diffusion and the diffusion through the product layer, which could be formed by iron minerals (maghemite and hematite). The apparent activation energy Ea was 19.5 kJ/mol.
2. The linear dependence of Sc extraction on Mg extraction was revealed. According to EPMA analysis, Sc in the raw RM is associated rather with Fe, and not with Mg. This

allows us to conclude that Mg acts as a leaching agent of Sc presented in the ion-exchangeable phase.

3. The pH has a significant effect on the Sc extraction degree. With a decrease in pH from 3.5 to 2, the Sc extraction after 90 min of leaching at $T = 70\text{ }^{\circ}\text{C}$ increases from 10 to 68%. A low pH value is necessary for the Mg leaching from aluminosilicates, as well as Sc from solid matrix of maghemite and iron minerals that was not destroyed at the alkali fusion of the raw bauxite.
4. The maghemite containing solid residue obtained after Sc leaching can be used as a functionalized material.

Author Contributions: Conceptualization, I.L. and A.S.; methodology, I.L.; validation, L.C., I.L.; formal analysis, A.S., D.V.; investigation, L.C., J.N., A.K.; resources, L.C., I.L.; data curation, A.K., I.L.; writing—original draft preparation, A.S., D.V., D.R.; writing—review and editing, A.S., D.V., D.R.; visualization, J.N., D.V.; supervision, L.C.; project administration, I.L.; funding acquisition, D.R. All authors have read and agreed to the published version of the manuscript.

Funding: This work was funded by State Assignment, grant № 075-03-2021-051/5. The methodology for analysis Sc content in acid solution by ICP-OES was funded by a Ministry of Science and Higher Education of the Russian Federation scientific topic № 0137-2019-0023. The EPMA analysis was funded by RFBR, grant № 20-38-90277.

Acknowledgments: The authors would like to recognize the assistance provided by Dmitry Zinovlev from Scientific Research Centre “Thermochemistry of Materials” of National University of Science & Technology (MISIS) (Moscow, Russia) for calculation the Eh-pH diagrams using HSC Chemistry 9.9 software and by Diana Manukovskaya from Tananaev Institute of Chemistry - Subdivision of the Federal Research Centre «Kola Science Centre of the Russian Academy of Sciences» Science Centre of Russian Academy of Sciences (Apatity, Russia) for English language editing of the article.

Conflicts of Interest: The authors declare no conflict of interest.

References

1. Kaußen, F.M.; Friedrich, B. Methods for Alkaline Recovery of Aluminum from Bauxite Residue. *J. Sustain. Metall.* **2016**, *2*, 353–364, doi:10.1007/s40831-016-0059-3.
2. Power, G.; Gräfe, M.; Klauber, C. Bauxite Residue Issues: I. Current Management, Disposal and Storage Practices. *Hydrometallurgy* **2011**, *108*, 33–45, doi:10.1016/j.hydromet.2011.02.006.
3. Liu, Z.; Li, H. Metallurgical Process for Valuable Elements Recovery from Red Mud—A Review. *Hydrometallurgy* **2015**, *155*, 29–43, doi:10.1016/j.hydromet.2015.03.018.
4. Winkler, D.; Bidló, A.; Bolodár-Varga, B.; Erdő, Á.; Horváth, A. Long-Term Ecological Effects of the Red Mud Disaster in Hungary: Regeneration of Red Mud Flooded Areas in a Contaminated Industrial Region. *Science of The Total Environment* **2018**, *644*, 1292–1303, doi:10.1016/j.scitotenv.2018.07.059.
5. Ruyters, S.; Mertens, J.; Vassilieva, E.; Dehandschutter, B.; Poffijn, A.; Smolders, E. The Red Mud Accident in Ajka (Hungary): Plant Toxicity and Trace Metal Bioavailability in Red Mud Contaminated Soil. *Environ. Sci. Technol.* **2011**, *45*, 1616–1622, doi:10.1021/es104000m.
6. Klauber, C.; Gräfe, M.; Power, G. Bauxite Residue Issues: II. Options for Residue Utilization. *Hydrometallurgy* **2011**, *108*, 11–32, doi:10.1016/j.hydromet.2011.02.007.
7. Liu, S.; Guan, X.; Zhang, S.; Xu, C.; Li, H.; Zhang, J. Sintering Red Mud Based Imitative Ceramic Bricks with CO₂ Emissions below Zero. *Materials Letters* **2017**, *191*, 222–224, doi:10.1016/j.matlet.2016.12.028.
8. Fu, Y.; Xiong, Z.Q. Red Mud Based Geopolymer and Its Forming Mechanism. *AMM* **2014**, *538*, 28–31, doi:10.4028/www.scientific.net/AMM.538.28.
9. Wang, L.; Sun, N.; Tang, H.; Sun, W. A Review on Comprehensive Utilization of Red Mud and Prospect Analysis. *Minerals* **2019**, *9*, 362, doi:10.3390/min9060362.

10. Shiryayeva, E.V.; Podgorodetskiy, G.S.; Malysheva, T.Ya.; Gorbunov, V.B.; Zavodyanyi, A.V.; Shapovalov, A.N. Effects of Adding Low-Alkali Red Mud to the Sintering Batch at OAO Ural'skaya Stal'. *Steel Transl.* **2014**, *44*, 6–10, doi:10.3103/S0967091214010173.
11. Trushko, V.L.; Utkov, V.A.; Bazhin, V.Yu. Topicality and possibilities for complete processing of red mud of aluminous production. №5 (227) (2017) **2017**, doi:10.25515/PMI.2017.5.547.
12. Beloglazov, I.; Savchenkov, S.; Bazhin, V.; Kawalla, R. Synthesis of Mg–Zn–Nd Master Alloy in Metallothermic Reduction of Neodymium from Fluoride–Chloride Melt. *Crystals* **2020**, *10*, 985, doi:10.3390/cryst10110985.
13. Savchenkov, S.; Kosov, Y.; Bazhin, V.; Krylov, K.; Kawalla, R. Microstructural Master Alloys Features of Aluminum–Erbium System. *Crystals* **2021**, *11*, 1353, doi:10.3390/cryst11111353.
14. Røyset, J.; Ryum, N. Scandium in Aluminium Alloys. *International Materials Reviews* **2005**, *50*, 19–44, doi:10.1179/174328005X14311.
15. Zinoveev, D.; Pasechnik, L.; Fedotov, M.; Dyubanov, V.; Grudinsky, P.; Alpatov, A. Extraction of Valuable Elements from Red Mud with a Focus on Using Liquid Media—A Review. *Recycling* **2021**, *6*, 38, doi:10.3390/recycling6020038.
16. Liu, Y.; Naidu, R. Hidden Values in Bauxite Residue (Red Mud): Recovery of Metals. *Waste Management* **2014**, *34*, 2662–2673, doi:10.1016/j.wasman.2014.09.003.
17. Zhou, K.; Teng, C.; Zhang, X.; Peng, C.; Chen, W. Enhanced Selective Leaching of Scandium from Red Mud. *Hydrometallurgy* **2018**, *182*, 57–63, doi:10.1016/j.hydromet.2018.10.011.
18. Suzdaltsev, A.V.; Pershin, P.S.; Filatov, A.A.; Nikolaev, A.Yu.; Zaikov, Yu.P. Review—Synthesis of Aluminum Master Alloys in Oxide-Fluoride Melts: A Review. *J. Electrochem. Soc.* **2020**, *167*, 102503, doi:10.1149/1945-7111/ab9879.
19. Rivera, R.M.; Ounoughene, G.; Borra, C.R.; Binnemans, K.; Van Gerven, T. Neutralisation of Bauxite Residue by Carbon Dioxide Prior to Acidic Leaching for Metal Recovery. *Minerals Engineering* **2017**, *112*, 92–102, doi:10.1016/j.mineng.2017.07.011.
20. Pepper, R.A.; Couperthwaite, S.J.; Millar, G.J. Comprehensive Examination of Acid Leaching Behaviour of Mineral Phases from Red Mud: Recovery of Fe, Al, Ti, and Si. *Minerals Engineering* **2016**, *99*, 8–18, doi:10.1016/j.mineng.2016.09.012.
21. Rychkov, V.; Botalov, M.; Kirillov, E.; Kirillov, S.; Semenishchev, V.; Bunkov, G.; Smyshlyaev, D. Intensification of Carbonate Scandium Leaching from Red Mud (Bauxite Residue). *Hydrometallurgy* **2021**, *199*, 105524, doi:10.1016/j.hydromet.2020.105524.
22. Pasechnik, L.A.; Skachkov, V.M.; Chufarov, A.Yu.; Suntsov, A.Yu.; Yatsenko, S.P. High Purity Scandium Extraction from Red Mud by Novel Simple Technology. *Hydrometallurgy* **2021**, *202*, 105597, doi:10.1016/j.hydromet.2021.105597.
23. Yatsenko, S.P.; Pyagai, I.N. Red Mud Pulp Carbonization with Scandium Extraction during Alumina Production. *Theor Found Chem Eng* **2010**, *44*, 563–568, doi:10.1134/S0040579510040366.
24. Petrakova, O.V.; Panov, A.V.; Gorbachev, S.N.; Klimentenok, G.N.; Perestoronin, A.V.; Vishnyakov, S.E.; Anashkin, V.S. Improved Efficiency of Red Mud Processing through Scandium Oxide Recovery. In *Light Metals 2015*; Hyland, M., Ed.; John Wiley & Sons, Inc.: Hoboken, NJ, USA, 2015; pp. 91–96 ISBN 978-1-119-09343-5.
25. Petrakova, O.V.; Kozyrev, A.B.; Suss, A.G.; Gorbachev, S.N.; Panov, A.V. Improved Technology of Scandium Recovery from Solutions of Bauxite Residue Carbonation Leaching. In *Light Metals 2019*; Chesonis, C., Ed.; The Minerals, Metals & Materials Series; Springer International Publishing: Cham, 2019; pp. 1407–1413 ISBN 978-3-030-05863-0.

26. Akcil, A.; Akhmadiyeva, N.; Abdulvaliyev, R.; Abhilash; Meshram, P. Overview On Extraction and Separation of Rare Earth Elements from Red Mud: Focus on Scandium. *Mineral Processing and Extractive Metallurgy Review* **2018**, *39*, 145–151, doi:10.1080/08827508.2017.1288116.
27. Ochsenkuehn-Petropoulou, M.; Tsakanika, L.-A.; Lymperopoulou, T.; Ochsenkuehn, K.-M.; Hatzilyberis, K.; Georgiou, P.; Stergiopoulos, C.; Serifi, O.; Tsopelas, F. Efficiency of Sulfuric Acid on Selective Scandium Leachability from Bauxite Residue. *Metals* **2018**, *8*, 915, doi:10.3390/met8110915.
28. Zhu, X.; Li, W.; Xing, B.; Zhang, Y. Extraction of Scandium from Red Mud by Acid Leaching with CaF₂ and Solvent Extraction with P507. *Journal of Rare Earths* **2020**, *38*, 1003–1008, doi:10.1016/j.jre.2019.12.001.
29. Yagmurlu, B.; Dittrich, C.; Friedrich, B. Effect of Aqueous Media on the Recovery of Scandium by Selective Precipitation. *Metals* **2018**, *8*, 314, doi:10.3390/met8050314.
30. Rivera, R.M.; Xakalashe, B.; Ounoughene, G.; Binnemans, K.; Friedrich, B.; Van Gerven, T. Selective Rare Earth Element Extraction Using High-Pressure Acid Leaching of Slags Arising from the Smelting of Bauxite Residue. *Hydrometallurgy* **2019**, *184*, 162–174, doi:10.1016/j.hydromet.2019.01.005.
31. Borra, C.R.; Pontikes, Y.; Binnemans, K.; Van Gerven, T. Leaching of Rare Earths from Bauxite Residue (Red Mud). *Minerals Engineering* **2015**, *76*, 20–27, doi:10.1016/j.mineng.2015.01.005.
32. Ochsenkühn-Petropulu, M.; Lyberopulu, Th.; Parissakis, G. Selective Separation and Determination of Scandium from Yttrium and Lanthanides in Red Mud by a Combined Ion Exchange/Solvent Extraction Method. *Analytica Chimica Acta* **1995**, *315*, 231–237, doi:10.1016/0003-2670(95)00309-N.
33. Anawati, J.; Azimi, G. Recovery of Scandium from Canadian Bauxite Residue Utilizing Acid Baking Followed by Water Leaching. *Waste Management* **2019**, *95*, 549–559, doi:10.1016/j.wasman.2019.06.044.
34. Reid, S.; Tam, J.; Yang, M.; Azimi, G. Technospheric Mining of Rare Earth Elements from Bauxite Residue (Red Mud): Process Optimization, Kinetic Investigation, and Microwave Pretreatment. *Sci Rep* **2017**, *7*, 15252, doi:10.1038/s41598-017-15457-8.
35. Shoppert, A.; Loginova, I.; Rogozhnikov, D.; Karimov, K.; Chaikin, L. Increased As Adsorption on Maghemite-Containing Red Mud Prepared by the Alkali Fusion-Leaching Method. *Minerals* **2019**, *9*, 60, doi:10.3390/min9010060.
36. Vind, J.; Malfliet, A.; Bonomi, C.; Paiste, P.; Sajó, I.E.; Blanpain, B.; Tkaczyk, A.H.; Vassiliadou, V.; Panias, D. Modes of Occurrences of Scandium in Greek Bauxite and Bauxite Residue. *Minerals Engineering* **2018**, *123*, 35–48, doi:10.1016/j.mineng.2018.04.025.
37. Zhang, N.; Li, H.-X.; Cheng, H.-J.; Liu, X.-M. Electron Probe Microanalysis for Revealing Occurrence Mode of Scandium in Bayer Red Mud. *Rare Met.* **2017**, *36*, 295–303, doi:10.1007/s12598-017-0893-x.
38. Borra, C.R.; Pontikes, Y.; Binnemans, K.; Van Gerven, T. Leaching of Rare Earths from Bauxite Residue (Red Mud). *Minerals Engineering* **2015**, *76*, 20–27, doi:10.1016/j.mineng.2015.01.005.
39. Rivera, R.M.; Ulenaers, B.; Ounoughene, G.; Binnemans, K.; Van Gerven, T. Extraction of Rare Earths from Bauxite Residue (Red Mud) by Dry Digestion Followed by Water Leaching. *Minerals Engineering* **2018**, *119*, 82–92, doi:10.1016/j.mineng.2018.01.023.
40. Levenspiel, O. *Chemical Reaction Engineering*; 3rd ed.; Wiley: New York, 1999; ISBN 978-0-471-25424-9.
41. Boltzmann Fitting Function 2021.
42. Chaikin, L.; Shoppert, A.; Valeev, D.; Loginova, I.; Napol'skikh, J. Concentration of Rare Earth Elements (Sc, Y, La, Ce, Nd, Sm) in Bauxite Residue (Red Mud) Obtained by Water and Alkali Leaching of Bauxite Sintering Dust. *Minerals* **2020**, *10*, 500, doi:10.3390/min10060500.
43. He, Q.; Qiu, J.; Rao, M.; Xiao, Y. Leaching Behaviors of Calcium and Aluminum from an Ionic Type Rare Earth Ore Using MgSO₄ as Leaching Agent. *Minerals* **2021**, *11*, 716, doi:10.3390/min11070716.

